



university of
 groningen

faculty of science
and engineering

Improved Performance of Current Sharing and Average Voltage Regulation in DC Microgrids

UNIVERSITY OF GRONINGEN

19-06-2019

Author:

Wouter Wijffels - s2575817

Supervisors:

Prof. dr. ir. J.M.A. Scherpen

Ir. T. Kousemaker

Dr. M. Cucuzzella

Abstract

This research integrates a proposed distributed control scheme into a model with two nodes. The control scheme is designed to achieve current sharing and average voltage regulation, which is successfully indicated in simulations. By introducing load modifications and introducing real system parameters, the performance of the proposed controller in terms of current sharing and average voltage regulation is evaluated. Simulations indicate that the proposed controller is robust to the real-life values of elements in the experimental setup and a more general ZIP-load. Experiments indicate that there exists inadequate overlap between the experimental model and the simulations to evaluate the performance of the controller in practice.

Contents

1	Introduction	1
2	Problem Formulation	2
2.1	Problem Context	2
2.2	Stakeholder Analysis	2
2.3	Model Description	3
2.3.1	Two-nodes Model	3
2.3.2	Buck Converter	4
2.3.3	Load	4
2.4	Mathematical Model	4
2.4.1	System Dynamics and Performance	4
2.4.2	Controller Dynamics	5
3	Design Goal	6
4	Design Science Approach	7
5	Methodology	8
6	Validation	8
7	Model Modifications	8
7.1	Experimental Setup	8
7.2	Load Modeling	9
7.2.1	Load Structure	9
7.2.2	Parameter Selection	9
7.2.2.1	Constant Impedance (Z)	10
7.2.2.2	Constant Current (I)	10
7.2.2.3	Constant Power (P)	10
8	Simulations	11
8.1	Simulink	11
8.1.1	Model	11
8.1.2	Load Implementation	11
8.1.3	Results	12
8.2	LTspice	13
8.2.1	Model	13
8.2.2	Controller Implementation	14
8.2.3	Load Implementation	15
8.2.4	Results	15
9	Experiments	16
9.1	Model Configuration	16
9.1.1	Overall Model	17

9.1.2	Load Simplification	17
9.1.3	Current Sensor	17
9.2	Controller Configuration	18
9.2.1	Control Panel	19
9.2.2	Controller Output Conversion	19
9.3	Measurements	19
9.3.1	Individual Nodes	19
9.3.2	Connected Nodes	19
9.3.3	Load Variations	20
9.3.4	Controller Implementation	20
10	Conclusion	20
11	Discussion	21
12	Appendices	22
12.1	A: System Overview	22
12.2	B: Calculations	26
12.2.1	Constant Impedance Load	26
12.2.2	LTspice Loads	26

1 Introduction

Today, the world's major energy resources (e.g. fossil fuel, nuclear and hydro) are generated as Alternating Current (AC) power and are transported over AC energy grids [McFadden, 2017]. The technically advanced and widely implemented AC networks currently have several benefits over Direct Current (DC) networks. For example, AC power is cheaper to generate and voltage levels are transformed with higher efficiency compared to DC networks [Yuan et al., 2016]. However, many of the reasons that led to the domination of AC networks are no longer valid because distributed energy sources (e.g. photovoltaic systems), modern electrical loads and energy storing systems work equally well with DC power and can be integrated with AC systems through converters [Kaushik and Pindoriya, 2014]. This is furthermore illustrated by two promises in power developments that indicate the benefits of integrating DC systems in the power network. Firstly, the performance of renewable energy sources can be increased significantly. For instance, the performance of photovoltaic systems can be improved by 25% because of the eliminated DC-AC-DC conversion waste and wind turbines benefit from increased reliability and less costs in DC configurations compared to AC generation [Moreno-Munoz, 2014]. Secondly, DC power is becoming the major energy source of modern electronics [Saeedifard et al., 2010]. Examples are the increasing interest in electric vehicles, mobile devices and low power electronic devices (e.g. lighting and household products). Taking the potential of efficient distributed power generation and changing power demand into account, localized DC networks - or DC microgrids - may finally be practical [Todd, 2009]. DC microgrids comprise power generation, electrical storage, power distribution and electronics consuming energy (e.g. lighting and TV's) [Todd, 2009]. Distributed DC microgrids have been described as flexible, intelligent and active power networks that improve system reliability, efficiency and increase the renewable energy sources integration [Mehrasa et al., 2015]. Implementations of distributed DC microgrids are proven to be successful in rural areas in India and provide power to over 40,000 households [Palit and Malhotra, 2015]. Despite the promising benefits of DC systems, considerable challenges in terms of control, protection and operational issues remain in the integration of distributed DC microgrids in the current power network [Saeedifard et al., 2010]. In distributed DC microgrids, distributed control schemes intend to affect operational conditioning by controlling key parameters such as current, voltage and power [Kumar et al., 2019]. Common converters in DC microgrids are buck and boost converters, that are controlled to counterbalance fluctuations in source voltage and ensure power is distributed equally by the sources of the system [Viswanatha and Venkata, 2018]. The exact regulation of voltages to desired levels remains complex, so a popular approach is to regulate instead the average value of voltages across the whole microgrid towards a global voltage set point. This method for voltage regulation is defined as 'global voltage regulation' [Nasirian et al., 2015]. A popular method for distributing the total demand among the generation nodes of the microgrid is achieved by designing the controllers that aim for proportional current sharing [Trip et al., 2018]. Recent research indicated that a proposed distribution control scheme achieved good performance average voltage regulation and current sharing in simulations, independent on the initial condition of the microgrid [Trip et al., 2018].

This Bachelor Integration Project (BIP) contributes to existing knowledge by providing system modifications and experimental results to the simulated performance of the distributed

control scheme proposed by Trip et al., 2018. More specifically, modifications to the system mimic the experimental system and modifications to the load in the circuit are discussed to achieve improved performance of average voltage regulation and current sharing. Performance is referred to as the accuracy of the proposed distributed control scheme compared with the experimental results. Additionally, controlling distributed systems requires independently operating subjects responding to the communication architecture [Ishihara and Fukuda, 2000]. Summarizing, this BIP indicates the robustness of the proposed control scheme with respect to load modifications and an experimental setup with a communication network that exchanges information on the generated currents .

2 Problem Formulation

Understanding the context of this BIP is vital, but offers a broad perspective on solutions to the problem. In this section, the problem of the research is translated into the model to indicate the focus of this BIP. Firstly, the problem is described to indicate the challenges of this report. Secondly, stakeholders are distinguished based on their interest and involvement in the research. Lastly, the components and working principle of the experimental model are described.

2.1 Problem Context

The problem of this research is that the effect of unmodeled system dynamics and uncertainties in system parameters for the model by Trip et al., 2018 are not known and might require the system to include modifications to the load and proposed controller. In the proposed model, the buck converter describes a linear relation between the control input and the output voltage. As a consequence, the buck converter has been neglected in simulations and the control input is used as input to the system. In experiments, the buck converter is included and might differentiate the system dynamics from simulations. Furthermore, it is expected that unmodeled system dynamics (e.g. resistors) and uncertainties in system parameters differentiate the practical performance of average voltage regulation and current sharing from performed simulations. Once the model is tested in experiments, the performance will be evaluated and improved according to the above mentioned system modifications.

2.2 Stakeholder Analysis

Stakeholders concerned with this research are distinguished based on their level of interest in the outcome of the project and ability to influence the experiments of the project. Ranking the stakeholders based on these parameters classifies them as primary stakeholders or secondary stakeholders. Stakeholders are not taken into account when their level of interest and their level of influence power are low. Primary stakeholders, with high levels on both parameters, are involved closely with the research. Secondary stakeholders, with only one parameter indicated as high, require consideration shown or their needs taken into account. The stakeholders of this research are:

1. Prof. dr. ir. J.M.A. Scherpen – she is chair of the DTPA lab of the University of Groningen. She has high influence power on the outcome of the project, since the research must contribute to the strong position of the University in the Control Engineering field. Furthermore, she is part of the research group that developed the proposed controller that is evaluated in this BIP. This indicates that Scherpen is a primary stakeholder.
2. Dr. M. Cucuzzella – he is a postdoc who has conducted multiple research projects on DC microgrids and is the daily supervisor of this research. In addition to Scherpen, Cucuzzella is a member of the research group that developed the proposed controller and is. His knowledge on the field of DC microgrids and his involvement in the research on the proposed controller indicate that he has a high level of influence power on the direction of the project. Therefore, Cucuzzella is considered as a primary stakeholder.
3. Ing. M. Stokroos – he is the manager of the DTPA laboratory equipment. He is concerned with the proper utilization of the equipment, illustrating high influence power on the experiments. However, he has no specific interest in the outcome of the project. As a result, Stokroos is listed as a secondary stakeholder.

2.3 Model Description

In this Integration Project, the model consists of the proposed controller and the experimental two-nodes setup that has been built and tested by Beudeker, 2019. The model is explained by indicating the components of the experimental model and the mathematics of the dynamics and performance indicators.

2.3.1 Two-nodes Model

The overall model includes two nodes - or distributed generation units - and a line that connects the nodes. Each node consists of a DC power source, a DC to DC buck converter, a current sensor, an inductor, a resistor, a capacitor, a modifiable load and a voltage sensor. The two nodes are connected by a dynamic resistive-inductive line. In figure 1 the experimental system is shown. Experiments on the system are performed by modifying the input variables, that are the duty cycle within the converter and the load of the system. Both input variables are explained in the next sections. Accordingly, performance measures are indicated by the output variables, measured by the current and voltage sensors.

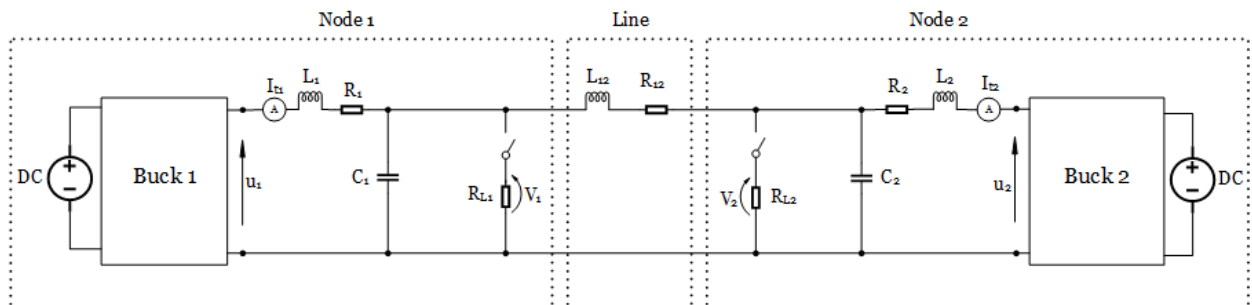


Figure 1: Model Description

2.3.2 Buck Converter

Each buck converter in figure 1 plays a vital role in the dynamics of the system by controlling the distributed amount of voltage over the system. As can be seen in figure 2, the controller input is the switch position (ON/OFF) inside the buck converter, which is the first input variable of the experiment. The ratio of the switch position, referred to as the duty cycle, represents the average dynamics of the control input. Since the relation between the output voltage and the duty cycle is linear, the model and the system are equivalent from a theoretical perspective. Therefore, the simulations assumed that control input u_1 and u_2 are considered as input voltages of the experimental system. In the experiments, current sensors on the nodes verify if this also holds in practice. To explain this theorem, the working principle of the buck converter is illustrated in figure 2 below.

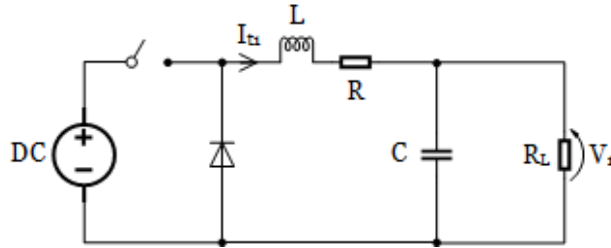


Figure 2: Working principle of the buck converter

2.3.3 Load

The load of the system is the second input variable of the experiment. Modifying the load affects the currents that are generated in the system. Trip et. al, 2018 established theoretical results by including only constant current loads in their model. Load modifications require the controller to accommodate to variations in the system to ensure it remains in accordance with the desired values. By measuring the response of the proposed controller in terms of generated currents and voltages in the nodes, the performance is indicated.

2.4 Mathematical Model

The system as described above is mathematically justified by Trip et al., 2018 and applied to the two-nodes setup of the experimental model. Firstly, this section elaborates on the mathematical formulation of the described model and performance measurements. Secondly, the controller dynamics and working principle of the controller are explained.

2.4.1 System Dynamics and Performance

Describing the system dynamics is carried out by the use of Kirchhoff's two formula's. Formula's 1 and 2 result from applying Kirchhoff's Current Law and indicate the steady state of the currents of the nodes. This law indicates that the sum of current in a junction equals zero. I_{t1} and I_{t2} indicate the current generated in the nodes that are measured by the current sensors. I_{L1} and I_{L2} are the current loads in the nodes that are modified later in the report. Formula's 3 and 4 are derived from using Kirchhoff's Voltage Law and describe the steady

state of the voltages in the node. This law explains that the sum of potential differences in a closed circuit equals zero. These laws describe the change of current and voltage of the system over time, that is referred to as the dynamic behaviour of the system. It can be seen that the dynamics depend on the controller output minus the voltage drops in the node and the load. Formula 5 describes the measured current between the nodes and subtracts the voltage drop over the line. A positive value indicates current flowing from node 1 to node 2 and a negative value indicates an opposed direction of current flow.

$$C_1 \dot{V}_1 = I_{t1} - I_{12} - I_{L1} \quad (1)$$

$$C_2 \dot{V}_2 = I_{t2} + I_{12} - I_{L2} \quad (2)$$

$$L_1 \dot{I}_1 = -R_{t1} I_{t1} - V_1 + u_1 \quad (3)$$

$$L_2 \dot{I}_2 = -R_{t2} I_{t2} - V_2 + u_2 \quad (4)$$

$$L_{12} \dot{I}_{12} = -R_{12} I_{12} + V_1 - V_2 \quad (5)$$

Concerning the quantification of performance, two control objectives are explained. Firstly, considering current sharing, the objective is to generate equal sharing of current between the two nodes. Mathematically, this means that the measured currents should converge to each other over time as can be seen in formula 6. In practice, this is unrealistic, so the lower the absolute difference, the higher the performance. Secondly, considering voltage regulation, the objective is to distribute voltages equal over the loads of the system according to a predetermined reference value. Over time, the smaller the difference between the average voltage and the reference voltage is, the higher the performance is, as shown in formula 7 below.

$$\lim_{t \rightarrow \infty} I_{t1} = \lim_{t \rightarrow \infty} I_{t2} = \frac{I_{L1} + I_{L2}}{2} = i_t^* \quad (6)$$

$$\lim_{t \rightarrow \infty} \frac{V_1 + V_2}{2} = V_{ref} \quad (7)$$

2.4.2 Controller Dynamics

The controller dynamics are described by a combination of state variables of the system and of the controller. Formula's 8 and 9 are dependent on the generated currents in the nodes and an edge weight that is equal for both nodes. Formula's 11 and 12 require the generated current in each node and the value ϕ . T_θ and T_ϕ are parameters that serve to tune the controller response. The controller output for the nodes consists of three terms as is illustrated by formula's 13 and 14. The first term helps fine tuning the controller output by decreasing the amount of oscillations, the second term stabilizes the system around desired values and the third term indicates the reference voltage that determines the value to which the average voltage among the nodes is regulated.

$$T_{\theta_1} \dot{\theta}_1 = \gamma(I_{t1} - I_{t2}) \quad (8)$$

$$T_{\theta_2} \dot{\theta}_2 = \gamma(I_{t2} - I_{t1}) \quad (9)$$

$$T_{\phi_1} \dot{\phi}_1 = -\phi_1 + I_{t1} \quad (10)$$

$$I_{t1,2}, \theta_{1,2}, \phi_{1,2} \quad (11)$$

$$T_{\phi_2} \dot{\phi}_2 = -\phi_2 + I_{t2} \quad (12)$$

$$u_1 = -K(I_{t1} - \phi_1) + \gamma(\theta_1 - \theta_2) + V_{ref} \quad (13)$$

$$u_2 = -K(I_{t2} - \phi_2) + \gamma(\theta_2 - \theta_1) + V_{ref} \quad (14)$$

It is important to notice that establishing the controller output does not require any voltage measurements from system. However, the distributed controllers prescribe a communication network to exchange information regarding the generated current. Below, this principle is visually explained in figure 3. Each distributed controller receives information respecting current measurements in the node (Y_1 and Y_2) and transmits the controller output (u_1 and u_2) back to the system to determine the duty cycle in the controller of each node. The dotted line represents the information shared between the nodes, as can be seen in formula's 8 - 14, that is crucial to achieve average voltage regulation and current sharing.

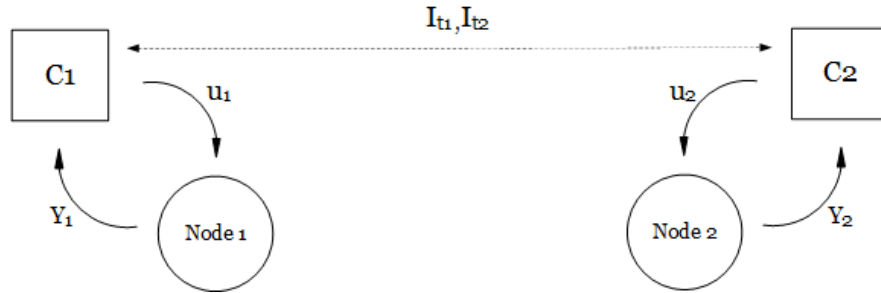


Figure 3: Working principle communication network

3 Design Goal

The goal of this Integration Project is to provide insights in average voltage regulation and current sharing in a DC microgrid with two nodes. In particular, to test the robustness of the proposed controller with respect to load modifications and the experimental setup. To achieve this goal, three design contributions are made in this research. Firstly, the proposed controller is modified towards the experimental setup wherefore it uses real-life system parameters that are determined by Beudeker, 2019. Secondly, load modifications are designed to subject the

proposed controller to more general loads (e.g. ZIP-loads). Since the proposed controller was subjected to constant current load, it is assumed that load modifications provide new insights in the behaviour of the controller that can help improve its performance. Lastly, the proposed controller is tested on the experimental setup. The experiments indicate how the controller is affected by unmodeled system dynamics and uncertainties in the system.

4 Design Science Approach

In the field of Design Science, theoretical approaches are proven to be helpful for determining appropriate research fields for the desired design goal. An important approach is the Three Design Cycles, that indicates to what research fields a project is contributing, as described by Hevner [Hevner, 2007]. Each cycle has its unique set of iterative steps and communicates with other cycles in terms of knowledge or requirement sharing.

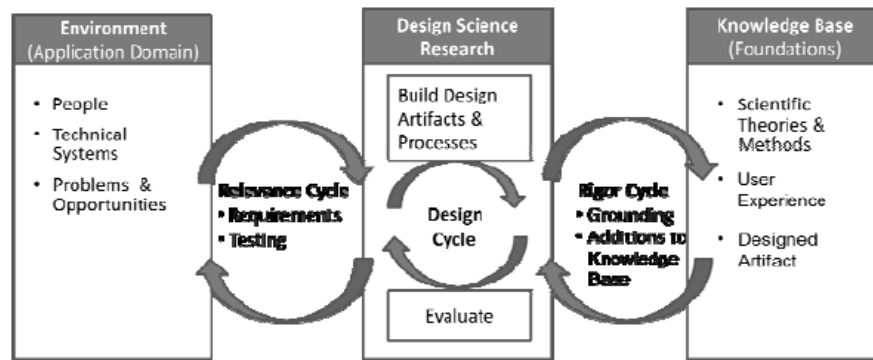


Figure 4: Hevner's Design Cycles

Firstly, figure 4 indicates that the Relevance Cycle is operating between the environment and Design Science Research. Its goal is to recognize the desired artifact. The cycle is initialized by understanding a specific need or demand, analyzing the situation and determining the artifact or construct that is most promising in satisfying the need or demand. Secondly, the Rigor Cycle is noticed to operate between Design Science Research and the knowledge base. Its goal is to gain novel phenomena on abstract levels. This cycle starts by the recognition to bridge a knowledge gap, evaluating knowledge and obtaining test results. Thirdly, the relation between cycles is described by the Design Cycle. This cycle gathers information from the Rigor Cycle and the need and want from the Relevance Cycle. Including this knowledge to the research contributes to designing and evaluating artifacts.

This BIP uses existing concepts from the knowledge base, performs experiments in the real environment and has the goal to design a model for improved performance of global voltage regulation and current sharing. Therefore, this project is determined to operate in the Design Cycle.

5 Methodology

The Design Cycle performs iterations between three methods to evaluate the performance of the proposed controller. Starting at the Rigor Cycle, mathematical models are proposed to prove the functioning of the system and controller. In 2.4 the formula's describe the system dynamics and are extended according to the system modifications. Subsequently, simulations test the models and bridge the gap between theory and practice. Simulations are performed implement the mathematical model in MATLAB and LTspice to predict the behaviour of the proposed controller in the experimental setup. The simulations use the setup as explained in the system description and include the proposed controller. The simulations are validated by Martin Stokroos, before implementing in the experimental setup since it is important to know what deviations from the simulations can be expected. Finally, once the simulations are approved by Martin Stokroos, the experimental setup is built. In this setup, unmodeled system dynamics and real-life noise are the point of interest. By modifying the load, different scenarios are evaluated and modifications are proposed to improve the performance of the model. These modifications can be translated in mathematics that proceed the iterative cycle of the methodology.

6 Validation

The research will be validated by evaluating the outcome of the methodologies. Validating the research is carried out by analyzing the outcome of the iterative steps of the methodology. The outcome will provide insights in the behavior of the controller in terms of predetermined modifications on system dynamics and unknown unmodeled system dynamics. Combining the insights helps adjusting the controller to improve the performance of current sharing and average voltage regulation.

7 Model Modifications

This chapter elaborates on the model modifications that are made with respect to the developed model. The first two contributions of this report require modifications to the model on which the proposed controller is tested. Required changes to imitate the experimental setup and the modifications to the load are explained. An important note is that the values that are assigned to system parameters and load in this section are used in the next chapters.

7.1 Experimental Setup

To predict the behaviour of the proposed controller in the experimental setup, the experimental setup of Beudeker, 2019 is used and revised. To start, the proposed controller is designed for n nodes and m lines and thus can be tuned easily to the setup of this research with $n = 2$ and $m = 1$. Next, the controller aims for both current sharing and average voltage regulation, in contrast to the PI controller of Beudeker, 2019 that exclusively aimed for voltage regulation. For the experimental setup, this requires a current sensor in both nodes that has a value of $0,1\Omega$. Additionally, the MOSFET in the experimental setup has an internal

resistance of 0.055Ω . Both resistors cause voltage drops in the nodes that must be taken into account. Furthermore, real system components are used for the inductor and capacitor in the nodes. By using the formula to calculate the peak-to-peak current ripple through the inductor, the minimum value for the inductor is calculated to as 1mH [Beudeker, 2019]. The value of the capacitor is determined by specifying the maximum Equivalent Series Resistance and assigns a value of $2,2\text{mF}$ to the capacitor [Beudeker, 2019].

7.2 Load Modeling

Load modeling has received more attention in recent years because of the renewable integration, demand-side management, and smart metering devices [Arif et al., 2018]. To improve the performance of the proposed controller, the response to load variations are evaluating by modeling a more general load. Load types are categorized as static or dynamic loads consisting of exponentials or polynomials [Shang et al., 2006]. To model a load, two steps are carried out: selecting the load structure and selecting the load parameters.

7.2.1 Load Structure

The selected load structure in this research is the ZIP-load. ZIP-loads are commonly used in both static and dynamic studies and consist of constant impedance (Z), constant current (I) and constant power (P) loads [Taylor, 1994]. In the setup of this research, the load parameters are varied over time, indicating a dynamic load model. In 2.4 the mathematical description of the system dynamics indicates that the voltage in the nodes is affected by the current I_{L1} and I_{L2} . In each node, the ZIP-load modifies the constant current load into a constant impedance load ($\frac{V}{R_L}$), constant current load (I_I) and constant power load ($\frac{P}{V}$). Formula's 15 and 16 below illustrate how the ZIP-load affects the system dynamics.

$$C_1 \dot{V}_1 = I_{t1} - I_{12} - \frac{V_1}{R_{L1}} - I_{I1} - \frac{P_1}{V_1} \quad (15)$$

$$C_2 \dot{V}_2 = I_{t2} - I_{12} - \frac{V_2}{R_{L2}} - I_{I2} - \frac{P_2}{V_2} \quad (16)$$

7.2.2 Parameter Selection

Formula's 15 and 16 describe the dynamic behaviour of the nodes with respect to the load. The voltage is measured over the capacitor in both nodes, and is, because of the load connected in parallel to the capacitor, equal to the voltage over the load. Regulating the voltage of the system requires the reference voltage and the voltages of both nodes. As a result, selecting the parameters of the load has instant effect on the currents generated in the nodes and average voltage regulated. Load modeling requires different values of the load to validate the response in terms of current sharing and average voltage regulation. However, the value of the current through the ZIP-load must be within the limits of the experimental setup. Below, an overview of the these values for each parameter is shown in table 1, and each parameter is briefly explained thereafter.

Time (ms)	Node 1			Node 2		
	Z	I	P	Z	I	P
0 - 100	$\frac{V_{out}}{10\Omega}$	10A	$\frac{10W}{V_{out}}$	$\frac{V_{out}}{0.5828\Omega}$	5A	$\frac{10W}{V_{out}}$
101 - 200	$\frac{V_{out}}{5\Omega}$	5A	$\frac{10W}{V_{out}}$	$\frac{V_{out}}{1.4285\Omega}$	10A	$\frac{10W}{V_{out}}$
201 - 300	$\frac{V_{out}}{1.4285\Omega}$	10A	$\frac{10W}{V_{out}}$	$\frac{V_{out}}{5\Omega}$	5A	$\frac{10W}{V_{out}}$
301 - 400	$\frac{V_{out}}{0.5828\Omega}$	5A	$\frac{10W}{V_{out}}$	$\frac{V_{out}}{10\Omega}$	10A	$\frac{10W}{V_{out}}$

Table 1: Overview of the parameters for the ZIP-loads

7.2.2.1 Constant Impedance (Z)

Constant impedance loads consist of an impedance, like a resistor. In this research four resistors are switched in parallel and have values of $R_1 = 10\Omega$, $R_2 = 10\Omega$, $R_3 = 2\Omega$ and $R_4 = 1\Omega$. The current always flows through the first resistor and additional resistors are connected to model parallel circuit modes. Four modes are tested, for which each subsequent mode another resistor is switched in parallel. The calculations for the total resistances are given in formulas 23, 24, 25 and 26 in the Appendix. From these calculations it follows that the corresponding values are $R_1 = 10\Omega$, $R_{12} = 5\Omega$, $R_{123} \approx 1.4285\Omega$ and $R_{1234} \approx 0.5882\Omega$. To express the constant impedance as current value, the output voltage is divided by the value of the total resistance.

7.2.2.2 Constant Current (I)

The constant current load draws approximately the same amount of current, regardless of variations in the source voltage or other resistors in the circuit. As for the constant impedance load, the value of the current drawn from the system can be adjusted, resulting in load steps over time. The currents and difference between the currents must be of significant size to indicate the controller's response. Therefore, the values of the current are tested in values of $I_I = 5A$ and $I_I = 10A$.

7.2.2.3 Constant Power (P)

The constant power load changes it's load on fluctuations of input voltage to keep the power constant. Hence, the constant power load uses the same input voltage as the constant impedance load. Ensuring the load is in line with the circuit, the constant arbitrarily value of $P = 10W$ is assigned to the constant power load.

8 Simulations

The simulations are performed in Simulink and LTspice to bridge the gap between theoretical knowledge and the experimental setup. Firstly, simulations in Simulink indicate how the controller responds to the mathematical model implemented in MATLAB. Secondly, LTspice continues simulations by introducing real-life components to accurately predict the behaviour of the system in experimental setup.

8.1 Simulink

Simulink elaborates on the first two contributions made in this research by implementing the system modifications as MATLAB functions into the block diagram in Simulink. Firstly, the proposed controller is adjusted to the experimental setup. Secondly, load modifications are tested to provide insights in the robustness of the controller.

8.1.1 Model

The model in this research builds on the Simulink and MATLAB model of Trip et al., 2018. In MATLAB, the parameters and dynamics of the system and controller are defined and checked for the two-nodes setup. As a modification, the real system parameters introduced in 7.2.2 and the reference voltage of 10V are set. In Simulink, the feedback loop from the output voltage is directed to the load current to integrate the ZIP-load. In figure 12 in the Appendix A the model of the system can be seen. On the left, the inputs of the state-space equations are the controller output and the load. On the right, the outputs are performance measurements indicating the voltages in the nodes, currents generated in the nodes and current flowing between the nodes.

8.1.2 Load Implementation

Implementing the loads as described in 7.2.2 is done by creating a load model in Simulink and introduce parameters in MATLAB to assign values to the load model. The loads of the nodes are altered over time to demonstrate the performance of the controller to load modifications. Therefore, the values of the loads have opposed values and are simulated in step functions, as can be seen in 5.

In 5, the ZIP-loads of both nodes are illustrated in a simulation of 20 seconds. The values of the load change every five seconds, as described in 7.2.2.

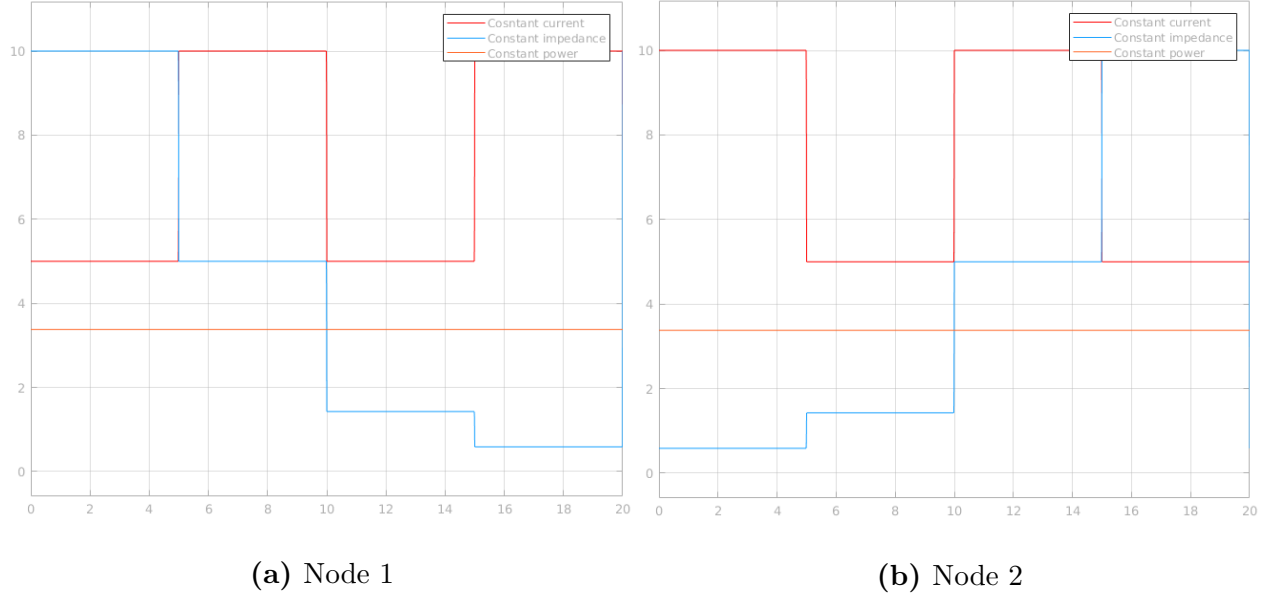


Figure 5: Current values of the ZIP-loads in Simulink

8.1.3 Results

The results of the simulations in Simulink including load modifications and parameters of the experimental setup as explained above are shown in 6 below that emphasize on the performance of the controller.

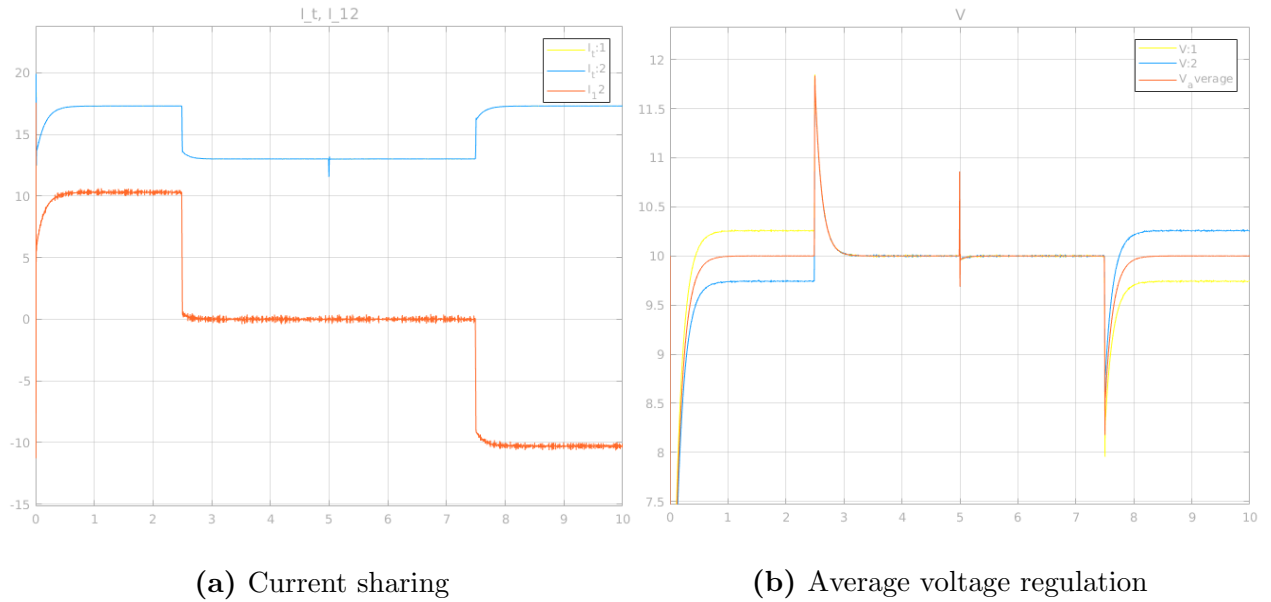


Figure 6: Performance of the Simulink simulations

In figure 6a, two graphs clarify the performance of current sharing. The two graphs of I_{t1} and I_{t2} show currents generated in the nodes and the current between the line of the nodes

is indicated below in the figure. As can be seen, the currents generated in the nodes, I_{t1} and I_{t2} , are approximately equal to each other, indicating good performance of current sharing according to formula 6. This is confirmed by the value of I_{12} , illustrating current is flowing between the nodes. A positive value indicates current flowing from node 1 to node 2, and negative values indicate flow in opposed direction. Figure 6b shows the voltages over the capacitor in each of the nodes and the average of these voltages. Large drops in voltage indicate larger peaks of the system to adjust itself to the new load. The voltages of the nodes have larger deviations, while the average remains in accordance with the reference voltage. Since the average voltage is in accordance with the reference voltage of 10V, formula 7 is satisfied and average voltage regulation in the system is achieved. Overall, it can be concluded that the controller achieves good performance in Simulink simulations. Both current sharing and average voltage regulation with respect to the modifications to the load and parameters of the experimental setup are achieved.

8.2 LTspice

8.2.1 Model

Different from the Simulink model, the LTspice model introduces real-life system components instead of a block diagram to simulate the system. As a result, the actual experimental setup is resembled by connecting all elements of the system with wires and assigning the real-life values to the components. The complete overview of this system is shown in figure 14 in Appendix A. Simplifying the system neglects implemented formula's and the controller, as shown below in figure 7. In this figure, the model predicts the behaviour of the model by simulating the experimental setup as real-life electric circuit. The source voltage is indicated as 12V and converted to lower voltages by the buck converter. A working electrical circuit requires all elements positioned according to the direction of current flow and all elements must be grounded, indicated by the lines in the bottom of the figure directing to the ground arrows. Furthermore, each node consists of the inductor, capacitor, current sensor and ZIP-load. Nonetheless, the values of these elements are as described in 7.1 deviate from the the values of the non-ideal elements introduced in LTspice, such that the behavior is simulated more accurately. The buck converter is designed by the microcontroller and MOSFET, determining the duty cycle, and the Shottky (MBR745) diode.

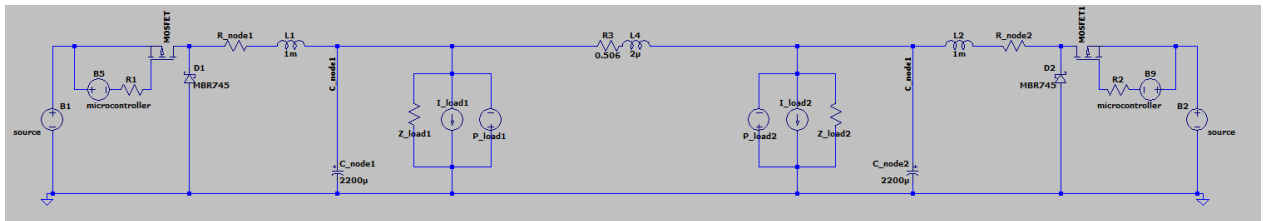


Figure 7: LTspice model of the two-nodes system

8.2.2 Controller Implementation

Implementing the controller in the model remains the most challenging aspect of the LTspice simulations. Compared to the proposed controller, a simplification and an addition are implemented to the controller output. As shown in formula's 13 and 14, the proposed controller is composed of three terms. Simulations in Simulink indicated that the controller achieves good performance with using all three terms on the experimental setup and load modifications. In contrast with Simulink, LTspice integrating the three terms does not lead to the desired results, hence modifications to the controller output are required. Each of the three terms is discussed, and if simplifications are required, these are explained.

The first term remains complicated to translate into working system elements in LTspice since ϕ uses a loop with values deviating from the mathematical model. Since this term does not affect the stability of the model, the controller output can be simplified by disregarding the first term. As a consequence, controller output as indicated by formula's 13 and 14 adopts $K = 0$ and results in formula's 18 and 18.

$$u_1 = \gamma(\theta_1 - \theta_2) + V_{ref} \quad (17)$$

$$u_2 = \gamma(\theta_2 - \theta_1) + V_{ref} \quad (18)$$

The second term depends on θ and uses the generated current of both nodes and scaling factor γ . To implement this term, the steady state equations of the controller dynamics are rewritten, as can be seen in 19 and 20. In LTspice, the arbitrary behavioural voltage source is used as element to introduce θ . This term allows using multiple measured variables as input, and creates a voltage term used by the controller output.

$$\theta_1 = \frac{-1}{T_{\theta_1}} \gamma \int (I_{t1} - I_{t2}) \quad (19)$$

$$\theta_2 = \frac{-1}{T_{\theta_2}} \gamma \int (I_{t2} - I_{t1}) \quad (20)$$

The third term is the reference voltage. For a working converter, the source voltage is decreased to the reference voltage, that is equal to the average voltage of the system as mentioned in 2.4.

Additions to the controller output are required due to modifications for simulating the experimental setup more accurately. Contrasting to Simulink simulations, the experimental setup uses a voltage source as input source instead of the controller output. The modification in LTspice integrates a buck converter in each of the nodes to control the system towards desired values. Beudeker, 2019 designed a buck converter with a P-channel MOSFET and Shottky diode as switches. Implementing the proposed controller in the buck converter is carried out by using the controller output to determine the switching behaviour of the MOSFET. The MOSFET is switched by Pulse Width Modulation (PWM) according to the sawtooth function for determining the duty cycle. However, this MOSFET has an internal resistance of $0,055\Omega$ causing a voltage drop in the buck converter. As a consequence, this voltage drop is compensated by the controller output.

8.2.3 Load Implementation

In LTspice load simulations have equivalent values of the loads designed in Simulink. However, LTspice does not use MATLAB to introduce functions to the system. Therefore, real components are used and if-statements determine the value of the load with respect to time. As mentioned in 7.2.1, the load values are summed, so the ZIP-load is designed in series. In this load, the constant current load is switched in opposed direction to drain current from the circuit. Figure 8 below provides an overview of the current load values for both nodes in a simulation of 400ms, where every 100ms the load switches to the subsequent mode corresponding to the values assigned in 7.2.2. In Appendix B the if-statements illustrate the ZIP-load working principle for LTspice.

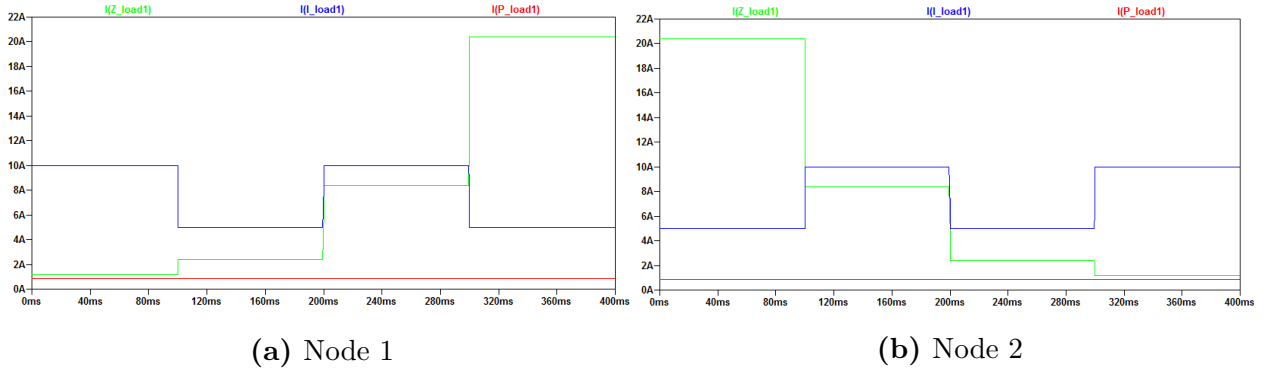


Figure 8: Current values of the ZIP-load in LTspice

8.2.4 Results

The results of LTspice are crucial for proceeding to the experiments since these are the closest approximation of the behaviour of the controller within the two-nodes setup. The results of the LTspice simulations are measured over a period of 400ms, indicating the four load variations. Towards experiments, it is important to predict the behavior of the controller on the reference voltage that is set in Simulink, and a lower value in accordance with the experimental setup. The first test evaluated the performance of the controller to the reference voltage of 10V and the second test illustrates the performance of the controller to a reference voltage of 5V. Figure 9 illustrates the performance of the proposed controller in terms of current sharing and average voltage regulation. Regarding figure 9a, the green and blue graph describe the currents generated in the nodes and the grey graph below indicates the current flowing over the line. It is noticeable that current sharing is achieved despite of the oscillations at the start of the simulation. Figure 9b indicates the average voltage regulation of the system. The voltages are measured over the capacitor in the nodes, which is parallel to the load, and the average of these values is indicated. It can be seen that the average voltage is in accordance with the reference voltage of 10V, indicating that average voltage regulation is achieved.

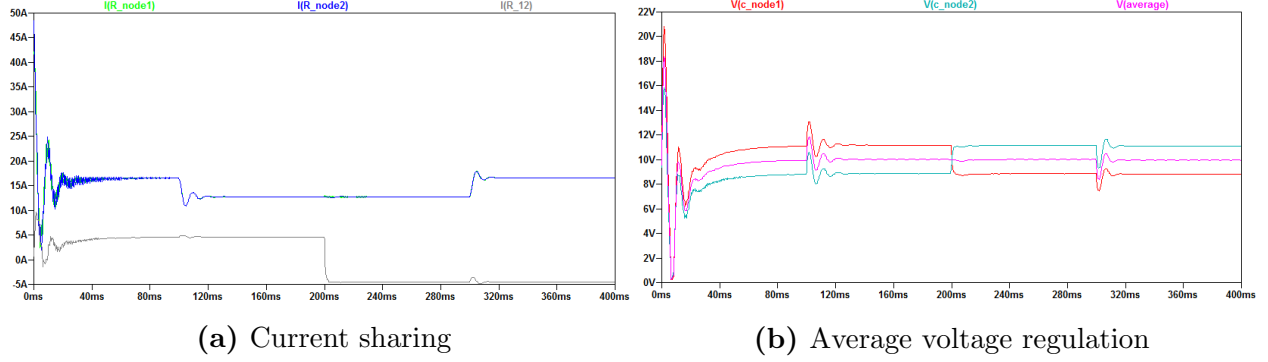


Figure 9: Performance with 10V reference

Nevertheless, the average voltage of the system is not immediately synchronized with the reference voltage. This notion, and the oscillations at the beginning of the generated current measurements, are explained by the fact that the first term of the controller output is neglected. In figure 10, the results of the simulation with 5V reference are shown. As can be seen, both current sharing and average voltage regulation are achieved with the reference of 5V. Moreover, the performance of voltage regulation is higher with the lower voltage reference since the average of the voltages converges faster to the reference voltage.

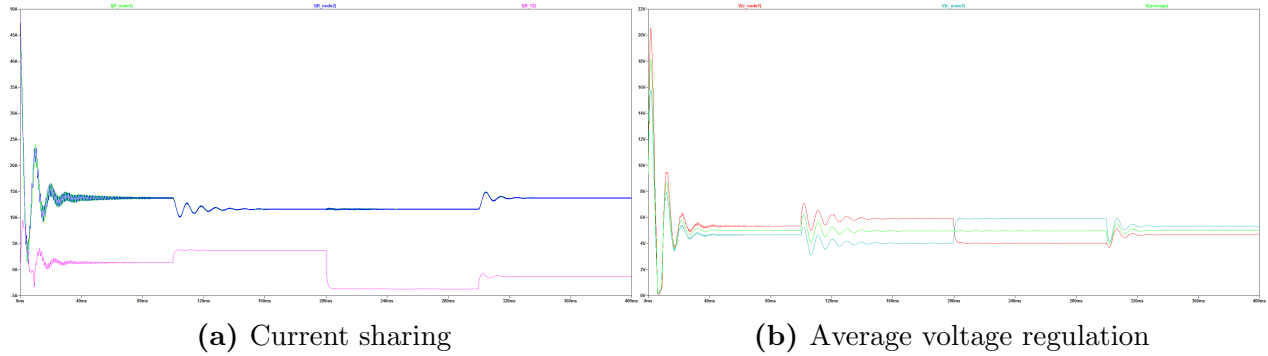


Figure 10: Performance with 5V reference

9 Experiments

The third and final contribution of this research concerns evaluating the behaviour of the proposed controller in experiments. This evaluation is carried out by reshaping the existing experimental setup of Beudeker, 2019, implementing the proposed controller and measurements its behaviour.

9.1 Model Configuration

This section elaborates on the elements are used to configure the experimental mode. Firstly, the overall model is defined. Secondly, the load model is described. Lastly, the working of the current sensor is explained.

9.1.1 Overall Model

The overall model for the experiments is based on the model as described in 2.3, with modifications to the experimental model that is built by Beudeker in 2019. Both nodes with corresponding loads and the Simulink Target Machine (STM) are shown in figure 16 of Appendix A. The STM is a device developed in the DTPA lab of the University of Groningen to integrate and test control schemes to devices. It is essential in the experiment because it sends the PWM to the nodes and receives the information concerning current and voltage measurements from the nodes. Behind the STM, the power source, oscillator and multimeter are positioned. The power source determines the source voltage for both nodes and indicates the current entering the circuit. The source visualizes these values with low accuracy, so the oscillator and multimeter are important to measure voltages more precisely. Lastly, M. Stokroos mentioned that the currents are expected to be relatively high for experimental setups. Therefore, the wires between the power source, between node and load and between the nodes are replaced lines with an increased thickness.

9.1.2 Load Simplification

In experiments, the load model is simplified towards the constant impedance load with values corresponding to 7.2.2. The reason to this design decision is twofold. Firstly, integrating the ZIP-controller in the experimental setup results in a complicated load model. Each parameter value must be connected to the STM, which will result in 7 STM signals for the load of each node. As a consequence, the number of wires between the STM and the nodes lead to an unclear setup. The experiments should be designed as simple as possible to indicate the uncertainties in the system. Since simulations in both LTspice and Simulink indicated that the controller is robust to load modifications, the experiments aim for the uncertainties in the elements of the nodes. Secondly, in contrast to LTspice, the experimental setup includes boundaries in terms of current and voltages. Simulations in LTspice indicate that with $V_{ref} = 5V$ and the constant impedance load, the nodes generate currents between 0A and 3A and the voltages remain between 3V and 6V, which is acceptable for the setup. As can be seen in figure 16 of Appendix A the load of node 1 is manually controlled by switches and the load of node 2 is controlled by signals send by the STM to activate the MOSFETs on the load model. The number of active resistors in node 2 and the period of the switching can be configured in Simulink.

9.1.3 Current Sensor

Current measurements must be send directly into the STM since the controller output relies on the currents generated in the nodes. To do this a current sensor is implemented on each node and connected to the STM as can be seen in 16 in Appendix A. The chosen current sensor is the INA 1x9 High-Side Current Shunt Monitor as shown below.

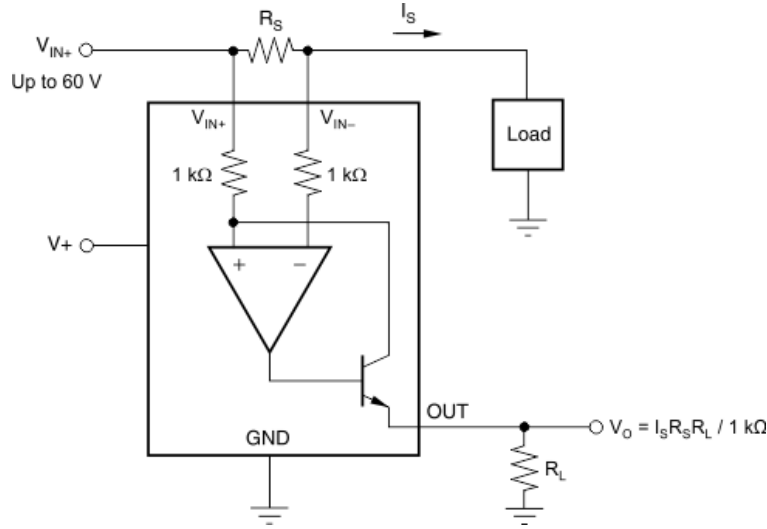


Figure 11: Overview of the current sensor design

This sensor measures the current next to the inductor in the circuit. It consists of a small sensor with resistor $R_s = 0,1\Omega$ over which a voltage is measured. This value is used to determine the resistor that is switched in parallel to the output voltage as can be seen in formula 21. Other values required by the formula are the approximated peak current and voltage of the node. These values are predicted by evaluating the LTspice simulation with $V_{ref} = 5V$, and the constant impedance load that will be used in the experimental setup. In accordance with this simulation, $I_s = 3A$ and $V_{out} = 6V$ are implemented in formula 22 below to determine R_L as $20k\Omega$. The current plotted in Simulink is calibrated by comparing values with measurements read from the multimeter. In subsequent tests, values of the current measures by hand in the nodes is in accordance with the currents shown in the plots of Simulink. Therefore, the currents sensor is implemented successfully and can be integrated with the proposed controller.

$$V_{out} = \frac{I_s R_s R_L}{1000\Omega} \quad (21)$$

$$R_L = \frac{V_{out} 1000\Omega}{I_s R_s} = \frac{6 * 1000}{3 * 0,1} = 20k\Omega \quad (22)$$

The current sensor automatically sends the measured current values to the STM once the model runs. However, the STM only reads voltages, so the voltage over the calculated resistor is measured and send as a signal of equivalent meaning into the STM.

9.2 Controller Configuration

Configuring the controller is carried out by integrating the digital control panel into the STM. Firstly, the elements of the control panel are explained. Secondly, the conversion of the controller output into the duty cycle is described.

9.2.1 Control Panel

Controlling the experimental setup is done by using a target file in Simulink. This target file receives the measurements of the voltages and currents in each node from the STM and sends the controller input as described in MATLAB functions and Simulink blocks. Figure 17 in Appendix A provides the overview of the control panel. On the left, the measured currents and voltages enter the STM and are converted to values appropriate for the scope and controller. On the right, the MOSFET switching of the resistances on node 2, indicated as R_{1234} in figure 16, is illustrated in the right bottom corner.

9.2.2 Controller Output Conversion

The same controller as introduced in the Simulink simulations, figure 13 appendix A, is implemented. In Simulink, all three terms of the controller worked successfully and are therefore implemented in the experimental model. As can be seen in 17, the controller receives measurements of the currents generated in the nodes and translates the controller output into the duty cycle, that is transmitted back into the experimental model. The controller output remains approximately within the voltage domain of the nodes, which is $0A - 12A$. The values of the controller output and modified by gain blocks and saturation to a value between -50 and 50 appropriate for the duty cycle. At the last two blocks on the right side, the data type is converted to the STM data type and transmitted to the STM.

9.3 Measurements

Measurements are step-wise carried out to test the working of all hardware components within the experiment. The model of Beudeker, 2019 is used as a setpoint for the experiments, all elements are thoroughly tested before implementing the controller. Firstly, the individual nodes and their response to PWM signals is tested. Secondly, both nodes and the line are connected and the circuit behavior is evaluated. Lastly, the proposed controller is implemented and tested on the circuit.

9.3.1 Individual Nodes

The first tests concern both controllers separately. The PWM signal received from the STM is measured and indicates that both MOSFETs accommodate to variations in duty cycles. These duty cycles are determined by using converted constant values. The constant values are within the value range of the proposed controller such that the duty cycle is simulated as accurate as possible. Furthermore, the currents between the nodes are evaluated precisely to avoid over stressing the setup. The tests on the nodes indicate that the current and voltage values of the nodes remain well within the dimensions of the nodes, indicating that the hardware of the nodes is installed correctly.

9.3.2 Connected Nodes

Both nodes indicated reliable responses such that they can be connected safely with the line. An ampere meter is positioned in the middle of the line to test whether the current over the

line flows in both directions. To test this, controller output constants are altered with respect to each other. For example, the controller output of node 1 is set to 3, while node 2 sets the controller output to 5. These values are translated into the PWM signal and measurements in the system are carried out. Interestingly, while implementing the same controller output to both nodes, there is a small current flowing over the line of $-60mA$. The explanation for this is that in the experiment, the nodes are not entirely balanced. Since the 10Ω resistors were initially not balanced equally in terms of power, a modification to the experiments is made to reduce this effect. As a result, the current flow over the line is reduced to $-30mA$. From these tests it is indicated that the currents flow over the line and modifying the duty cycle shows the predicted outcome.

9.3.3 Load Variations

The next step tests the response of the model to load variations. Values for the duty cycle remain constant to indicate the specified effect of the loads. Varying the total resistance of both nodes between R_1 , R_{12} , R_{123} and R_{1234} indicates current flowing between the nodes and the current between $0A - 1,8A$, which is within the current domain of $0A - 3A$. Since the measurements of voltages and currents of the load variations indicate that the system remains within the current and voltage boundaries, modifications to the duty cycle are included. Varying the constant controller output indicates that the hardware is controllable with load variations.

9.3.4 Controller Implementation

Implementing the controller is the most crucial part of the experiments. The current measurements of the sensor are integrated into the input streams of the controller and the output of the controller is converted to the duty cycle. Roughly said, the controller output is expected to indicate values between 0 and 12V. In the experiments, the measured values are within this domain. However, the current in the nodes is increased when implementing the controller. In one experiment the current caused the overheating of a MOSFET that required replacement. With a new MOSFET, the experiments are revised and the conductivity of the nodes is increased by soldering the bottom of the nodes and introducing aluminum plates attached to the MOSFET increasing the heat dissipation. Unfortunately, the controller remains unable to meet the control objectives to set average voltage in accordance with the reference voltage and generate equal currents.

10 Conclusion

The conclusion of this research is drawn by elaborating on the three contributions. Firstly, simulations in both Simulink and LTSpice indicate that the proposed controller achieves good performance of current sharing and average voltage regulation with respect to the experimental setup. This is an important step towards testing the controller in experiments by including new elements and altering elements to non-ideal values. The measured values illustrate that the system safely operates between the domain of $0 - 12V$ and $0 - 3A$ of the experimental setup. Secondly, in addition to performance of the controller on a constant current load, the

robustness with respect to a more general ZIP-load is illustrated in simulations. Thirdly, the experiments indicate that there is inadequate overlap between the simulations and experiments to achieve the control objectives in experiments. Despite functioning hardware and the working proposed controller, possible explanations for this indicate that there exist other aspects influencing the working of the controller such as differences in sampling time and specific limitations of circuit elements.

11 Discussion

This BIP provided new insights in the robustness of the proposed controller by introducing load modifications and real-life system parameters. For future research, four important challenges remain. Firstly, the system parameters of the experimental setup must be altered to bridge the gap between simulations and experiments. Secondly, ZIP-loads can be implemented in the experimental setup by using two STMs. Thirdly, more complex loads can be used to improve the response of the proposed controller to load modifications. Lastly, power sharing is an interesting in DC microgrids and future research can indicate whether this controller is also applicable to achieve good performance.

12 Appendices

12.1 A: System Overview

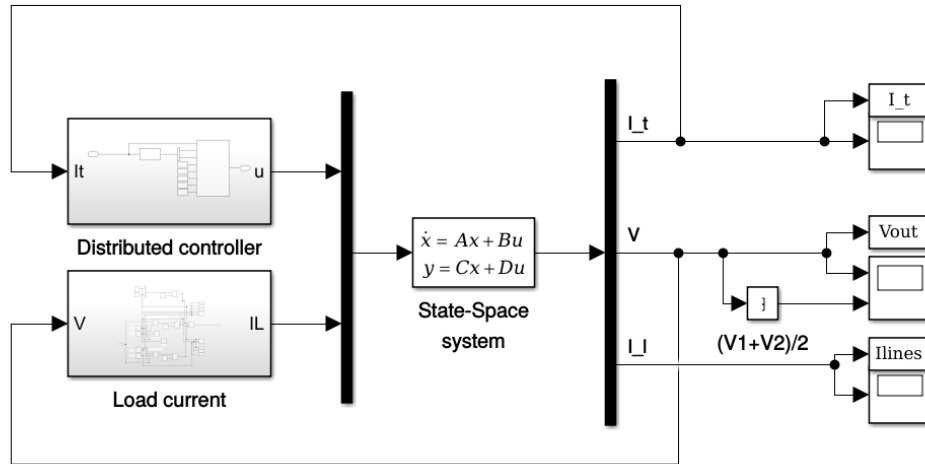


Figure 12: Setup of the complete system in Simulink

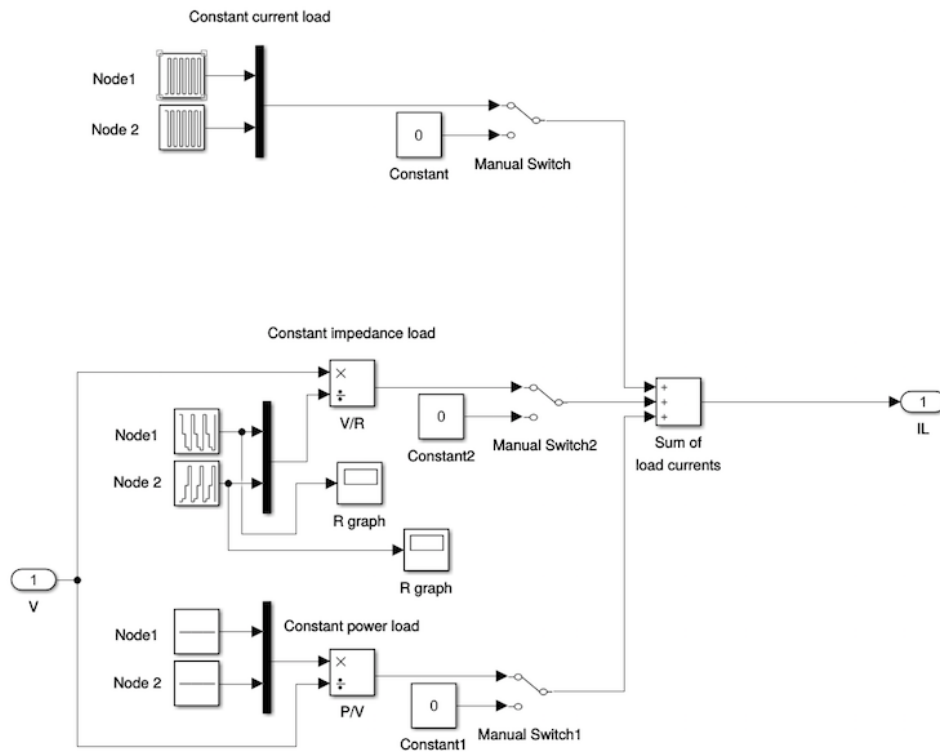


Figure 13: Setup of the ZIP-load current in Simulink

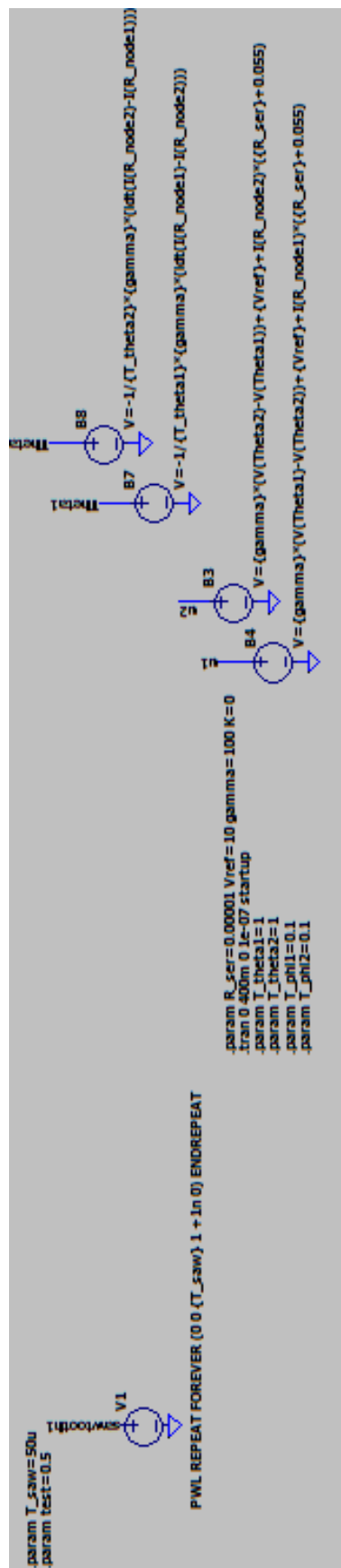
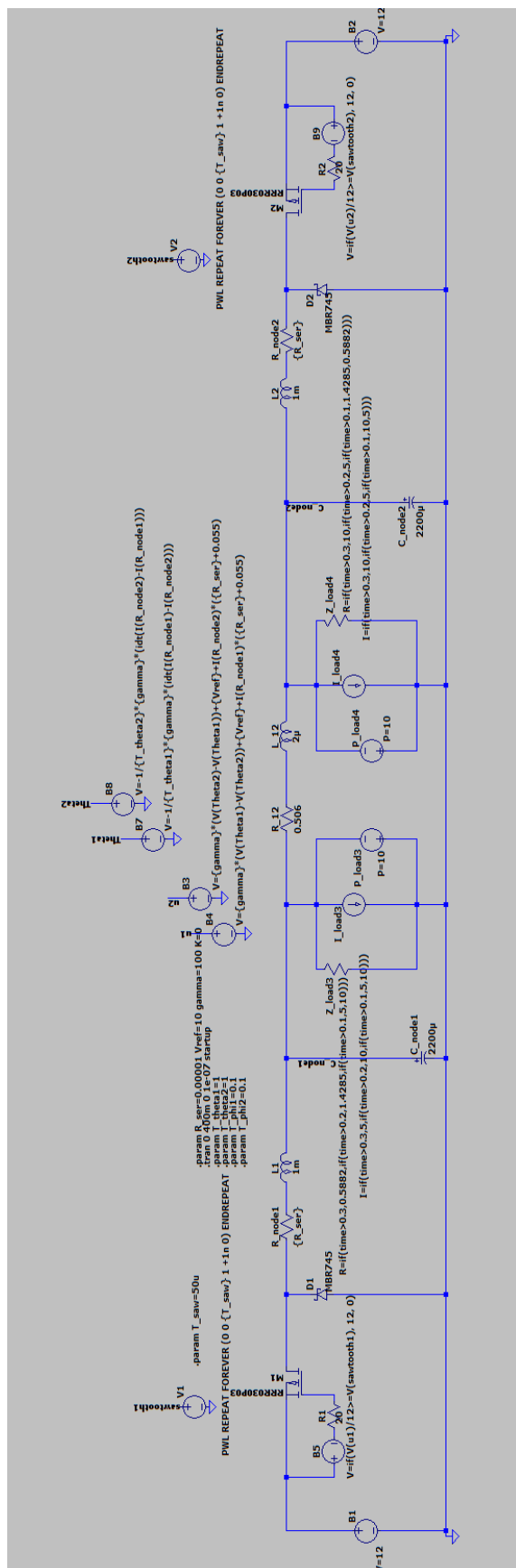


Figure 15: Setup of the controller in LTspice

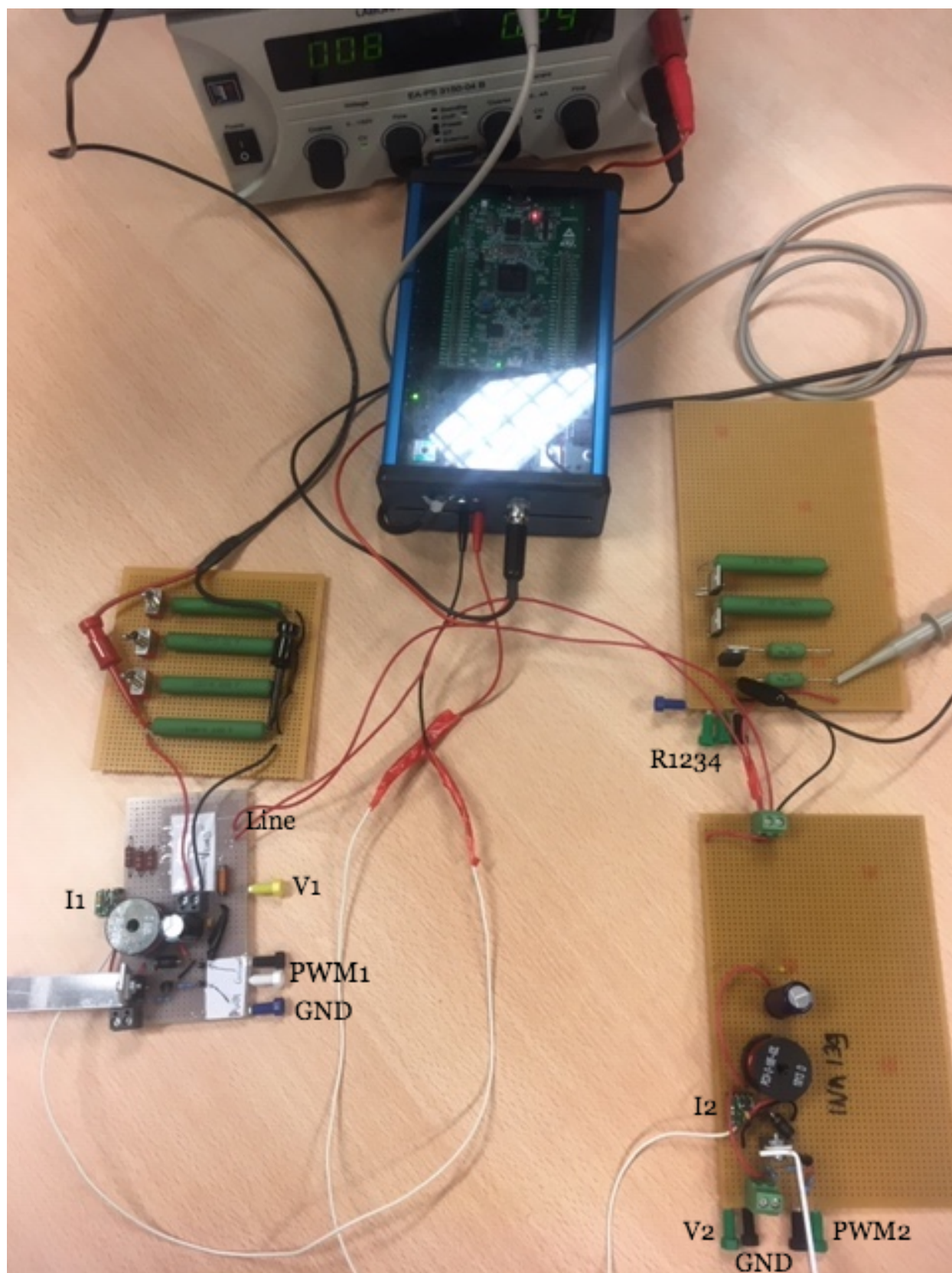


Figure 16: Experimental setup linked to the STM

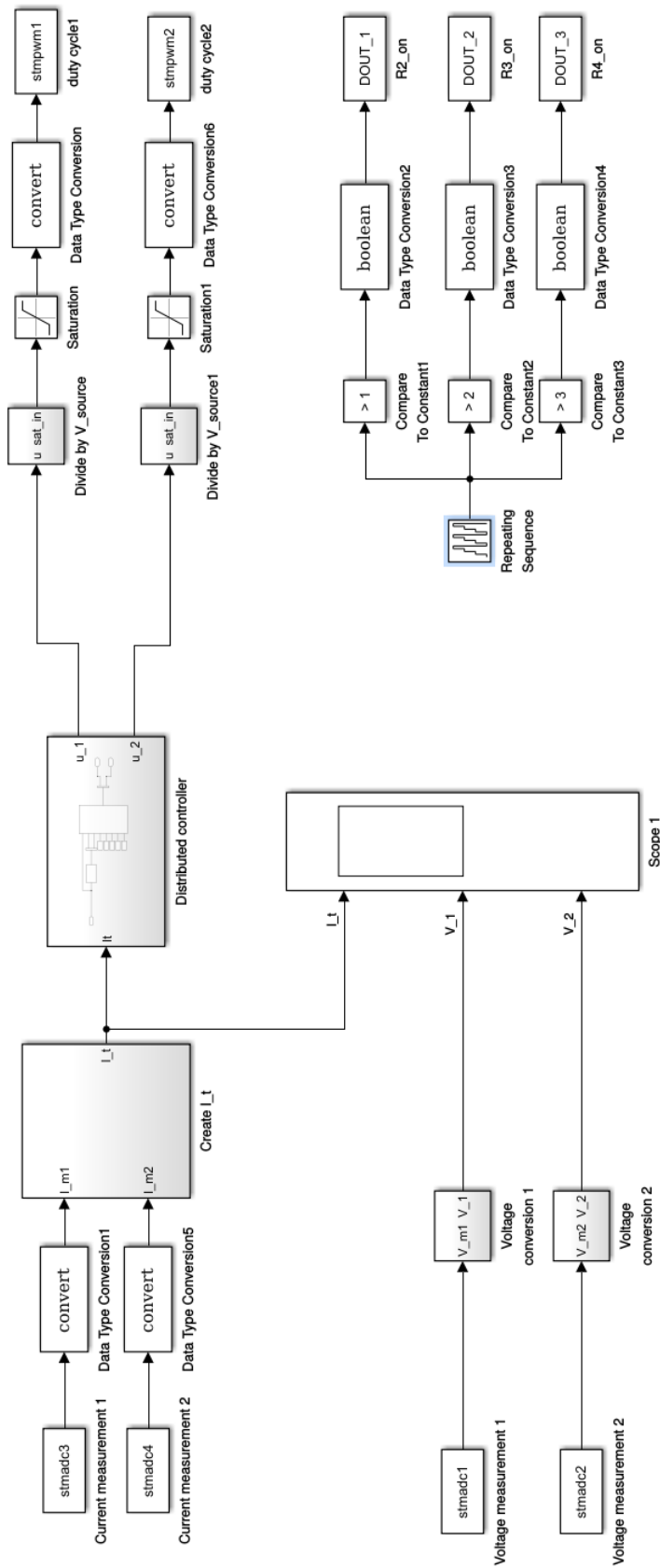


Figure 17: Setup of the control panel for the experiments in Simulink

12.2 B: Calculations

12.2.1 Constant Impedance Load

$$R_1 = 10\Omega \quad (23)$$

$$R_{12} = \frac{R_1 R_2}{R_1 + R_2} = \frac{10 * 10}{10 + 10} = \frac{100}{20} = 5\Omega \quad (24)$$

$$R_{123} = \frac{R_1 R_2 R_3}{R_3(R_1 + R_2) + R_1 R_2} = \frac{10 * 10 * 2}{2(10 + 10) + 10 * 10} = \frac{200}{140} \approx 1.4285\Omega \quad (25)$$

$$R_{1234} = \frac{R_1 R_2 R_3 R_4}{R_1 R_2 R_3 + R_3 R_4(R_1 + R_2) + R_1 R_2 R_4} = \frac{10 * 10 * 2 * 1}{200 + 2(20) + 100} = \frac{200}{340} \approx 0.5882\Omega \quad (26)$$

12.2.2 LTspice Loads

Node 1

$$R = \text{if}(t > 0.3, 0.5882, \text{if}(t > 0.2, 1.4285, \text{if}(t > 0.1, 5, 10))) \quad (27)$$

$$I = \text{if}(t > 0.3, 5, \text{if}(t > 0.2, 10, \text{if}(t > 0.1, 5, 10))) \quad (28)$$

$$P = 10 \quad (29)$$

Node 2

$$R = \text{if}(t > 0.3, 10, \text{if}(t > 0.2, 5, \text{if}(t > 0.1, 1.4285, 0.5882))) \quad (30)$$

$$I = \text{if}(t > 0.3, 10, \text{if}(t > 0.2, 5, \text{if}(t > 0.1, 10, 5))) \quad (31)$$

$$P = 10 \quad (32)$$

References

- [Arif et al., 2018] Arif, A., Wang, Z., Wang, J., Mather, B., Bashualdo, H., and Zhao, D. (2018). Load modelinga review.
- [Beudeker, 2019] Beudeker, S. (2019). Control of a dc to dc buck converter. unpublished thesis.
- [Hevner, 2007] Hevner, A. R. (2007). A three cycle view of design science research. *Scandinavian Journal of Information Systems*, 19.
- [Ishihara and Fukuda, 2000] Ishihara, H. and Fukuda, T. (2000). *Handbook of Sensors and Actuators*, volume 8.
- [Kaushik and Pindoriya, 2014] Kaushik, R. A. and Pindoriya, N. M. (Mar 2014). A hybrid ac-dc microgrid: Opportunities key issues in implementation. pages 1–6. IEEE.
- [Kumar et al., 2019] Kumar, J., Agarwal, V., and Agarwal, A. (2019). A review on overall control of dc microgrids. *Journal of Energy Storage*, 21:113–138.
- [McFadden, 2017] McFadden, C. (2017). All of the world’s energy generation systems in one list.
- [Mehrasa et al., 2015] Mehrasa, M., Pouresmaeil, E., Mehrjerdi, H., Jrgensen, B. N., and Catalo, J. P. S. (2015). Control technique for enhancing the stable operation of distributed generation units within a microgrid. *Energy Conversion and Management*, 97:362–373.
- [Moreno-Munoz, 2014] Moreno-Munoz, A. (2014). Ac vs. dc power a new battle of the currents.
- [Nasirian et al., 2015] Nasirian, V., Moayedi, S., Davoudi, A., and Lewis, F. L. (2015). Distributed cooperative control of dc microgrids. *IEEE Transactions on Power Electronics*, 30(4):2288–2303.
- [Palit and Malhotra, 2015] Palit, D. and Malhotra, S. (2015). Energizing rural india using micro grids: The case of solar dc micro-grids in uttar pradesh state, india.
- [Saeedifard et al., 2010] Saeedifard, M., Graovac, M., Dias, R. F., and Iravani, R. (2010). Dc power systems: Challenges and opportunities. In *IEEE PES General Meeting*, pages 1–7.
- [Shang et al., 2006] Shang, J., Zhang, J., and Li, S. (2006). Study on static voltage stability assessment for load center area. *2006 International Conference on Power System Technology*.
- [Taylor, 1994] Taylor, C. W. (1994). *Power system voltage stability*. McGraw-Hill.
- [Todd, 2009] Todd, B. (2009). Dc microgrids: a new source of local power generation?
- [Trip et al., 2018] Trip, S., Han, R., Cucuzzella, M., Cheng, X., Scherpen, J., and Guerrero, J. (2018). Distributed averaging control for voltage regulation and current sharing in dc microgrids: Modelling and experimental validation. *IFAC PapersOnLine*, 51(23):242–247.

- [Viswanatha and Venkata, 2018] Viswanatha and Venkata (2018). Microcontroller based bidirectional buckboost converter for photo-voltaic power plant. *Journal of Electrical Systems and Information Technology*, 5(3):745–758.
- [Yuan et al., 2016] Yuan, X., Liu, D., and Li, Q. (2016). Construction costs and transmission efficiency comparison of ac and dc distribution system.